Electrochimica Acta 134 (2014) 347–354

Contents lists available at ScienceDirect

Electrochimica Acta

journal homepage: www.elsevier.com/locate/electacta

Performance improvement of $LiCoO_2$ by MgF_2 surface modification and mechanism exploration

Ying Bai[a,*], Kai Jiang[a], Shuwei Sun[a], Qing Wu[a], Xia Lu[b], Ning Wan[a]

[a] Key Laboratory of Photovoltaic Materials of Henan Province and School of Physics & Electronics, Henan University, Kaifeng 475004, PR China
[b] Department of Mining and Materials Engineering, McGill University, Montréal (Québec) H3A2B2, Canada

ARTICLE INFO

Article history:
Received 22 February 2014
Received in revised form 16 April 2014
Accepted 27 April 2014
Available online 4 May 2014

Keywords:
Surface modification
Electrochemical performance
Solid electrolyte interface (SEI) film
Lithium ion batteries (LIBs)

ABSTRACT

$LiCoO_2$ cathode material synthesized by a sol-gel method is modified by different contents of MgF_2 via simple chemical deposition. The structure and morphology of pristine and MgF_2-coated $LiCoO_2$ are investigated by X-ray diffraction (XRD), field emission scanning electron microscopy (FESEM) and high resolution transmission electron microscopy (HRTEM). It is found that the homogeneous MgF_2 surface modification does not change the bulk structure of $LiCoO_2$. The effects of MgF_2 on the electrochemical behaviors of $LiCoO_2$ are studied. Comparatively, 1 wt.% MgF_2-coated $LiCoO_2$ exhibits the best electrochemical performances. Cyclic voltammetry (CV) results confirm that MgF_2 surface coating decreases the electrode polarization and improves the structural stability of $LiCoO_2$ during cycling. The results of electrochemical impedance spectroscopy (EIS) and Fourier transform infrared (FTIR) for pristine and 1 wt.% MgF_2-coated $LiCoO_2$ further demonstrates that modification layer suppresses the undesirable growth of solid electrolyte interface (SEI) film, which greatly contributes to the improved electrochemical performances after surface modification. Differential scanning calorimetry (DSC) tests show that MgF_2 coating also improves the thermal stability of $LiCoO_2$ electrode.

© 2014 Elsevier Ltd. All rights reserved.

1. Introduction

Lithium ion batteries (LIBs) have become the dominant power sources for portable electronic devices. Most recently, the fast development of hybrid electric vehicles (HEVs), electrical vehicles (EVs) and energy storage apparatus set higher and higher demand on their energy sources [1,2]. To meet the requirements of higher capacity and longer cycle life for LIBs, many researchers are focusing on the development of the cathodes working at higher potentials, including traditional electrode materials [3].

As the most commercialized cathode material for LIBs, $LiCoO_2$ is typically charged up to 4.2 V *versus* Li^+/Li and delivers a specific capacity of 140 mAh g^{-1}, although it has a high theoretical capacity of 274 mAh g^{-1}. In order to obtain higher capacity, it needs to be charged above 4.2 V [4–6].

However, the capacity fading of $LiCoO_2$ is quite pronounced under elevated upper cutoff voltage. Some research groups reported that the poor cycling performance above 4.2 V is attributed to structural instability and/or irreversible phase transition from a hexagonal phase to a monoclinic phase with accompanying volume change of ~2.6% along *c*-axis [7,8], which causes the accumulation of stress and propagation of microfractures in positive electrode, resulting in fast capacity decay with cycling [2,9].

Surface modification of $LiCoO_2$ with metal oxides and metal phosphates such as Al_2O_3, MgO, ZnO, ZrO_2, $AlPO_4$, $FePO_4$ and YPO_4 has been approved to successfully improve its cycling performance at higher voltage [10–12]. Sun *et al.* observed AlF_3 on the surface of Al_2O_3 coated active material with time of flight secondary ion mass spectrometry (ToF-SIMS) [13]. Bai *et al.* reported that the conversion of YPO_4 to YF_3 even happened in chemical storage of YPO_4 coated $LiCoO_2$ [14]. Inspired by their pioneering work, Lee *et al.* coated AlF_3 and LaF_3 on the surface of $LiCoO_2$, effectively improves the electrochemical performances of $LiCoO_2$ [15]. Enlightened by the previous studies, metal fluorides are most likely to be the ultimate products which make genuine contribution in repeated electrochemical cycling, and the improvement mechanism by metal fluoride modification has not been thoroughly elucidated up to now.

MgF_2 is widely applied in the design and development of various optical thin films and multilayer photonic crystals for its properties including high hardness, good thermal stability, low refractive index, higher transmissivity in the ultraviolet, visible and infrared range, low absorption and wide bandgap. Cho *et al.* coated MgF_2 on the surface of $LiCoO_2$ through dry-coating method and obtained

* Corresponding author. Tel.: +86 0371 23881602; fax: +86 378 3881 602.
E-mail addresses: ybai@henu.edu.cn, wonspring@126.com (Y. Bai).

http://dx.doi.org/10.1016/j.electacta.2014.04.155
0013-4686/© 2014 Elsevier Ltd. All rights reserved.

improved electrochemical performances, which were attributed to the reduced side reactions with electrolytes based on electrochemical impedance spectroscopy (EIS) analysis [16]. In their work, the coating process was quite complex and highly dependent on apparatus. Besides, the optimum proportion of MgF_2 in the coated cathode was not provided [16]. Lee *et al.* characterized the electrochemical properties of pristine and MgF_2 coated $LiCoO_2$ films, and contributed the electrochemical performance improvement of $LiCoO_2$ film to the protective effect MgF_2 coating layer only based on the analysis of Co dissolution [17]. In both of these two previous works, the influence of MgF_2 on the $LiCoO_2$ has not been comprehensively evaluated and the improvement mechanism has not been intensively explored yet.

In this paper, $LiCoO_2$ was modified by MgF_2 via simple chemical deposition, which is workable in practical application. The comparison of electrochemical performances show that electrode of $LiCoO_2$ coated by 1 wt.% MgF_2 exhibits the optimal cycling stability. Besides, it is found that the thermal stability of $LiCoO_2$ electrode has been improved by MgF_2 surface modification. Further, the mechanism for the improvements has also been intensively studied.

2. Experimental

2.1. Sample preparation

$LiCoO_2$ cathode material was synthesized by a sol-gel method. In a typical experiment, certain amount of lithium nitrate, cobalt nitrate and citric acid with molar ratio of 1.1:1:3.15 were separately put into three beakers and dissolved in distilled water to form transparent solutions with stirring. Next, the solutions were homogeneously mixed and the pH value was adjusted to 7.0 by slowly adding ammonia solution, followed by stirring at 80 °C for 5 h to form a sol. The sol was then thoroughly dried to form corresponding gel at 120 °C for 12 h. Afterwards, the gel was annealed at 750 °C for 4 h in air and naturally cooled down to room temperature, finally yielding black powder of $LiCoO_2$.

To prepare MgF_2-coated $LiCoO_2$, ammonium fluoride (Aldrich) and magnesium nitrate nonahydrate (Aldrich) were separately dissolved in distilled water. After that, the as-prepared $LiCoO_2$ powder was added into the magnesium nitrate nonahydrate solution in which the pH value was also adjusted to 7.0. The molar ratio of Mg to F was adjusted to be 1:2 and the amount of MgF_2 in the solution varied from 0 wt.%, 0.5 wt.%, 1 wt.% and 3 wt.%. The solution containing $LiCoO_2$ was constantly stirred at 80 °C for 5 h and repeatedly filtered by distilled water. Finally, the obtained powders were heated at 400 °C for 5 h in air.

2.2. Physical characterizations

The X-ray diffraction (XRD) patterns of the as-prepared $LiCoO_2$ samples were measured on Bruker D8 Advance diffractometer (Bruker, Germany) with Cu Kα radiation of $\lambda \sim 0.15418$ nm. In addition, the structural parameters were refined by the Rietveld method from XRD data with a 2 theta range from 10° to 130° using the Fullproof software. Morphological characterizations were carried out on a field emission scanning electron microscopy (FESEM) (JEOL 7001F). Electron diffraction spectroscopy (EDS) mapping was measured to determine the element distribution together with SEM in large field of view. The image of high resolution transmission electron microscopy (HRTEM) was collected on JEOL JEM 2010 equipment to investigate the sample microstructure. The inductively coupled plasma (ICP) analysis was performed on Thermo Fisher ICAP 6300 to determine the exact chemical compositions of the samples. Fourier transform infrared (FTIR) measurements were performed on Nicolet AVATAR360. Differential scanning calorimetry (DSC) analysis was carried out on TA Q600 by sealing the charged cathode (4.5 V at galvonostatic 0.1 C) in an Al crucible in dry Ar and heated from 100 to 350 °C at a rate of 5 °C min^{-1}.

2.3. Electrochemical characteristics

The working electrodes were fabricated by compressing the mixture of 84 wt.% active materials (pristine, 0.5 wt.%, 1 wt.%, 3 wt.% MgF_2-coated $LiCoO_2$), 8 wt.% acetylene black (Super-P, MMM Carbon) and 8 wt.% binder (polyvinylidene fluoride, PVDF), which were all dissolved in N-methyl-pyrroline (NMP) on an aluminum foil. After thoroughly dried, the films were cut into electrode sheets (8×8 mm^2) as working electrodes. 1 M $LiPF_6$ dissolved in a mixture of ethylene carbonate (EC) and dimethyl carbonate (DMC) with volume ratio of 1:1 was used as electrolyte. The assembly process was

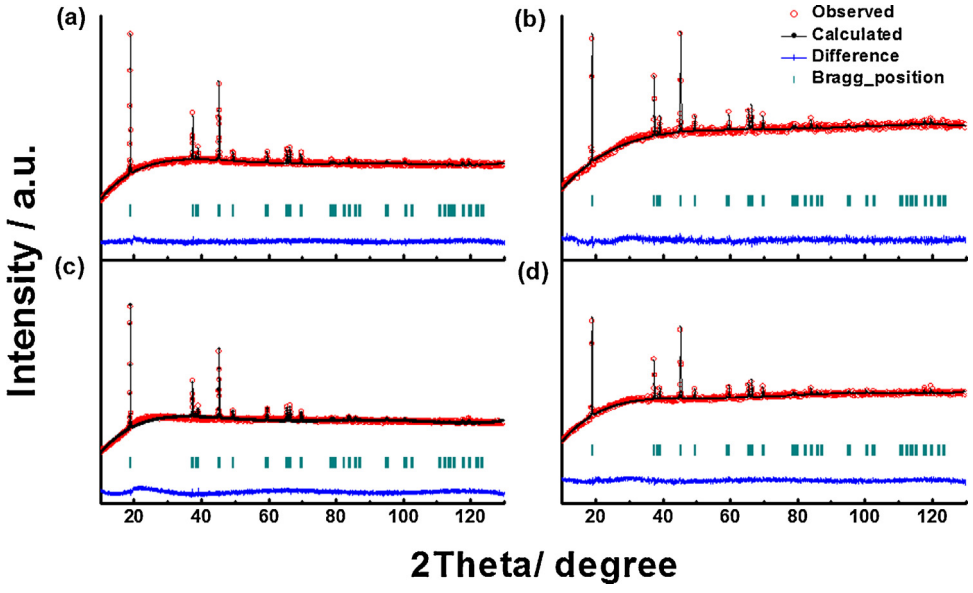

Fig. 1. Refined XRD patterns of pristine (a), 0.5 wt.% (b), 1 wt.% (c) and 3 wt.% (d) MgF_2-coated $LiCoO_2$ samples, which demonstrate that the collected XRD patterns show slightly difference with the simulated ones as confirmed to hexagonal $LiCoO_2$ phase.

conducted in an argon-filled glove-box with H_2O and O_2 content less than 1 *ppm*.

Before electrochemical tests, the batteries were sufficiently aged to ensure good soakage. The cells were charged and discharged on a battery tester (NEWARE CT-3008W-5V1 mA, China) between 3.0 and 4.5 V (*versus* Li^+/Li). Cyclic voltammetry (CV) and electrochemical impedance spectroscopy (EIS) investigations were performed on an electrochemical workstation with three electrode systems (CHI660 C, Shanghai). The CV curves were recorded between 3.0 and 4.5 V at a scan rate of 0.05 mV s^{-1}. The EIS measurements were performed over a frequency range from 100 kHz to 5 mHz.

3. Results and discussion

3.1. Physical characteristics

Fig. 1 shows the XRD patterns of pristine and MgF_2-coated $LiCoO_2$ powders. All the powders are confirmed to be well-defined hexagonalα-$NaFeO_2$ structure with a space group of $R\bar{3}m$ [18]. No diffraction peaks can be assigned to the MgF_2 phase in the obtained XRD patterns. Rietveld refinement is performed to obtain the structural parameters of the samples, and the results are listed in Table 1. The unit cell parameter *a*, an indication of the metal-metal distance within the (001) layer [19], displays negligible variations after surface coating. Besides, the *c/a* value reveals the extent of trigonal distortion [19]. As shown in Table 1, a high *c/a* value 4.99, which is desirable for better hexagonal structure for layered compounds [20], also remains the same. The high *c/a* values and the

Table 1
Structural parameters of the pristine and MgF_2-coated $LiCoO_2$ powders.

Sample	*a* (Å)	*c* (Å)	Volume (Å^3)	*c/a*
pristine	2.814(4)	14.046(9)	96.35	4.9911
0.5 wt.% MgF_2	2.814(2)	14.045(6)	96.33	4.9910
1 wt.% MgF_2	2.814(5)	14.044(2)	96.34	4.9899
3 wt.% MgF_2	2.814(2)	14.045(5)	96.33	4.9909

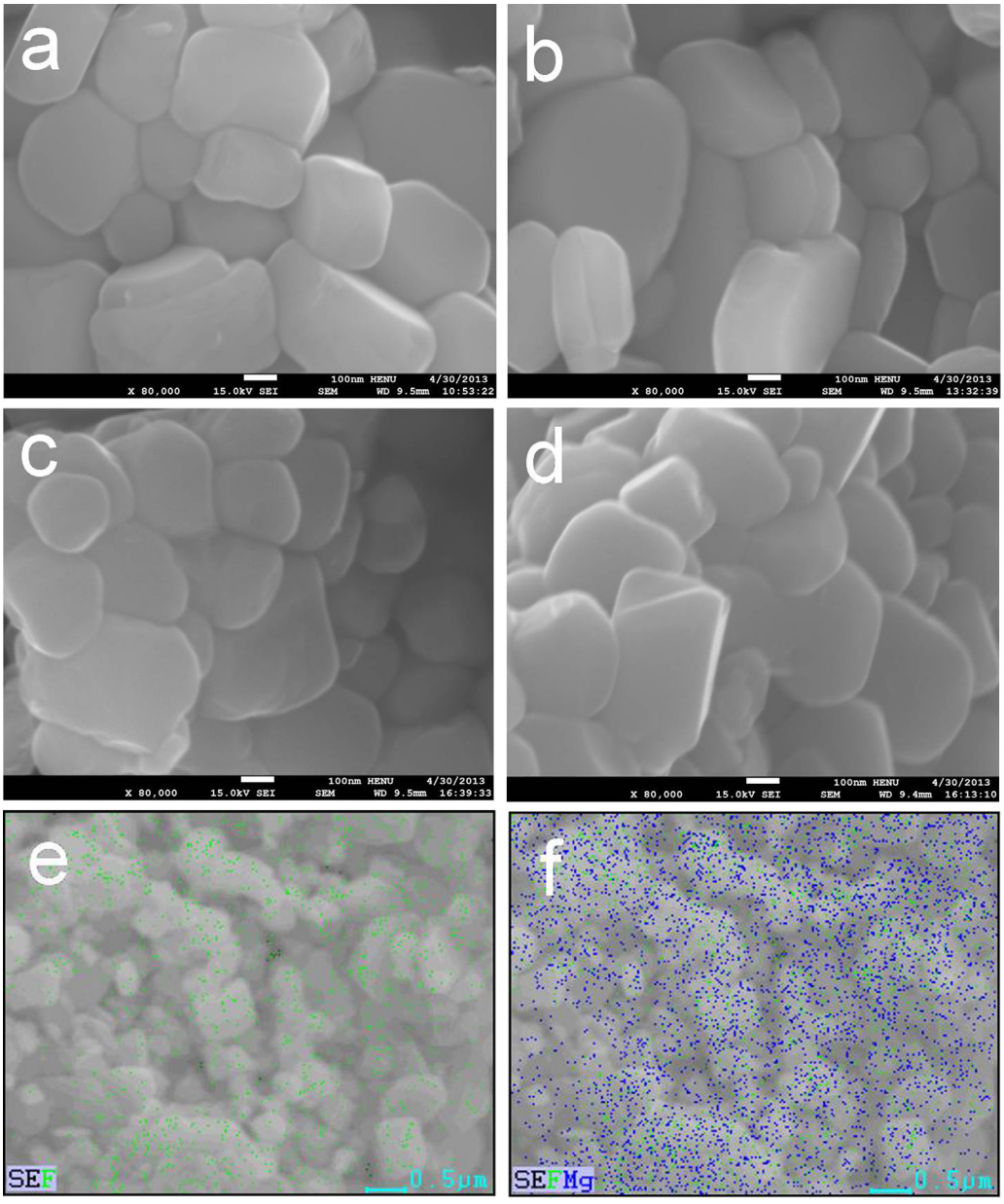

Fig. 2. Surface morphologies of pristine (a) 0.5 wt.% (b) 1 wt.% (c) and 3 wt.% (d) MgF_2-coated $LiCoO_2$ and EDS mappings of F (e) and Mg (f) for 1 wt.% MgF_2-coated $LiCoO_2$.

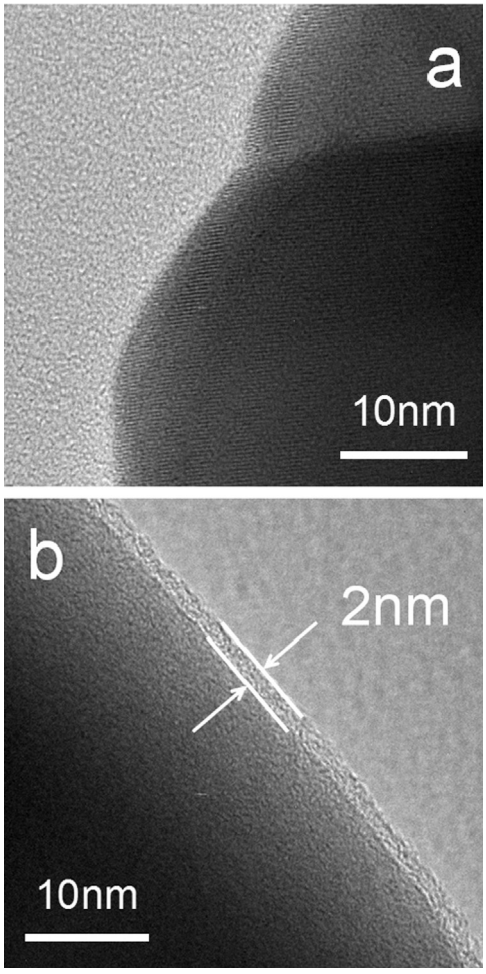

Fig. 3. TEM of (a) pristine and (b) 1 wt.% MgF_2-coated $LiCoO_2$.

well-resolved splitting of the XRD peaks assigned to the pairs of Miller indices (006)/(102) and (108)/(110) in all the compounds are good indications of a nearly perfect hexagonal layered structure [21]. No obvious change of the lattice parameters could be observed among the four samples, implying that the structure of $LiCoO_2$ remains unchanged after MgF_2 surface modification.

SEM images of the pristine and MgF_2-coated $LiCoO_2$ are shown in Fig. 2. The particles of pristine $LiCoO_2$ are uniformly distributed, with smooth and clean surface, as can be observed in Fig. 2(a). The particle size keeps unchanged after surface modification with different contents of MgF_2 (Fig. 2(b)-(d)). Careful investigation indicate that the surfaces and edges gradually become obscure with increasing amount of coating, showing a thin layer outside $LiCoO_2$ exists after MgF_2 modification. Fig. 2(e) and (f) present the EDS mapping images for 1 wt.% MgF_2-coated $LiCoO_2$. It is clearly observed that F and Mg are evenly distributed, indicating that the MgF_2 layer deposited outside the $LiCoO_2$ particle surface is homogeneous.

To directly observe the microstructure of MgF_2 coating layer, TEM images were recorded and compared. Fig. 3 reveals the TEM images of the pristine and 1 wt.% MgF_2-coated $LiCoO_2$. It is apparent that the pristine $LiCoO_2$ is well crystallized, with lattice fringe extending to the grain boundary (Fig. 3(a)). The crystal orientation can be clearly viewed along (003), corresponding with the XRD results. Not surprisingly, the 1 wt.% MgF_2-coated $LiCoO_2$ material (Fig. 3(b)) exhibits an amorphous and uniform modification layer with thickness of about 2 nm on the surface. This modification layer

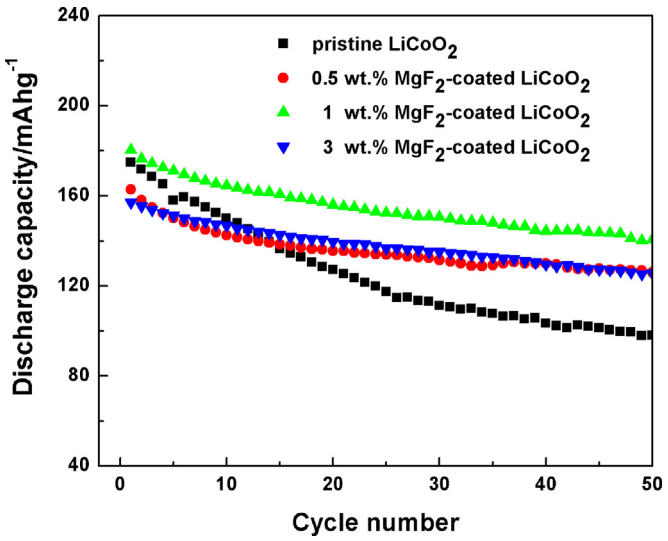

Fig. 4. Comparison of capacity retentions for pristine and MgF_2-coated $LiCoO_2$ between 3.0 and 4.5 V at 0.2 C rate.

of MgF_2 will separate the direct contact between the electrode and electrolyte and thus suppress side reaction(s).

ICP analysis was also conducted to determine the exact content of MgF_2 in the coated materials. It shows that the actual contents of MgF_2 are 0.39 ± 0.01, 0.76 ± 0.01 and 2.35 ± 0.01 wt.% for 0.5, 1 and 3 wt.% MgF_2-coated $LiCoO_2$. Nevertheless, we still call 0.5, 1 and 3 wt.% MgF_2-coated $LiCoO_2$ in the following discussion.

3.2. Electrochemical characteristics

The influence of MgF_2 coating layer on the capacity retention of $LiCoO_2$ in the range of 3.0-4.5 V at a current rate of 54.8 mA g^{-1} (0.2 C) is compared in Fig. 4. Apparently, pristine $LiCoO_2$ suffers fast capacity decay with cycling. It releases an initial discharge capacity of 175 mAh g^{-1}, while after 50 cycles, it sharply decreases to 98 mAh g^{-1}, with capacity retention of only 56%. As can be clearly observed in Fig. 4, MgF_2 surface modification greatly improves the cyclability of $LiCoO_2$. Comparatively, 1 wt.% MgF_2 coating is the most effective in improving the cycling performance of $LiCoO_2$. The initial discharge capacity is about 180 mAh g^{-1}, which still remains 141 mAh g^{-1} after 50 cycles, with high capacity retention of 80%. The cycling performance gets worse when the MgF_2 content increases from 1 wt.% to 3 wt.%, implying that excessive MgF_2 coating plays a negative role in the transportation of Li^+, which could be attributed to the intrinsic chemical and electrochemical inactivity of it.

Fig. 5 shows the discharge capacities of pristine and 1 wt.% MgF_2-coated $LiCoO_2$ cells at various current densities between 3.0 and 4.5 V. The discharge capacity of pristine $LiCoO_2$ drops dramatically with increasing current. Comparatively, 1 wt.% MgF_2-coated $LiCoO_2$ delivers higher discharge capacities and shows slower capacity decay at high current, indicating that MgF_2 coating effectively improves the rate performance of $LiCoO_2$. Furthermore, the discharge capacity can be completely recovered when the current density is reset to 0.2 C, implying that the 1 wt.% MgF_2-coated $LiCoO_2$ electrode experienced high rate cycling still retains good electrochemical reversibility and structural stability.

When the cell is charged to a higher potential, larger amount of Co^{3+} will convert to Co^{4+} in $LiCoO_2$ structure. If the cathode material is exposed to electrolyte, the strong oxidizing Co^{4+} will attack the carbonate groups of the solvent due to their nucleophilic properties and are easily reduced to Co^{3+} or Co^{2+} [22]. Simultaneously, Co^{4+} ions are capable of oxidizing alkyl carbonates to produce CO_2

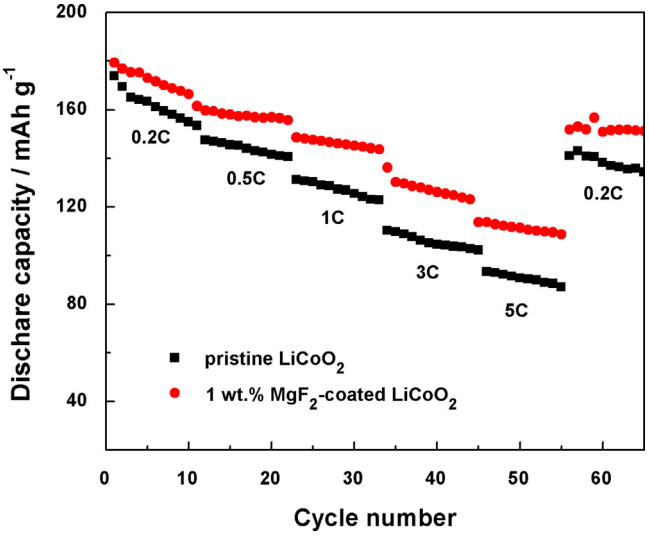

Fig. 5. Comparison of rate performances for pristine and 1 wt.% MgF_2-coated $LiCoO_2$.

Table 2
Redox potentials and D-Values of pristine and MgF_2-coated $LiCoO_2$.

Cycle number	Redox potential (V)		D-Value (V)[a]	
	pristine	1 wt.% MgF_2	pristine	1 wt.% MgF_2
1st	3.92/3.87	3.93/3.89	0.05	0.04
	4.08/4.05	4.07/4.05	0.03	0.02
	4.17/4.14	4.17/4.15	0.03	0.02
2nd	3.94/3.86	3.94/3.88	0.08	0.06
	4.09/4.05	4.08/4.05	0.04	0.03
	4.18/4.14	4.18/4.13	0.04	0.03

[a] D-value: difference between redox pairs.

[22], resulting in the formation of various organic species at the interfaces [23]. Accordingly, these surface films may be the main sources for impedance increasing [16] and main reason for capacity decay [24]. It is confirmed that the coating layer of MgF_2 efficiently prevented the dissolution of Co^{4+} and successfully protected the surface of the electrode from the reactive electrolyte [17]. The uniform MgF_2 coating layer herein can effectively prevent Co^{4+} from direct contact and reaction with the electrolyte, which contributes to the stabilization of $LiCoO_2$ and decreases the side reactions in cycling. This partly explains the enhanced capacity retentions in Figs. 4 and 5.

In order to explore the mechanism of electrochemical performance improvement of MgF_2 coating layer on $LiCoO_2$, CV profiles were collected and presented in Fig. 6. For pristine $LiCoO_2$, a well-defined current redox at 3.92/3.87 V with a long tail is observed in the initial cycle, corresponding to the complex solid-solution reaction. The oxidation peaks at 3.92, 4.08 and 4.17 V are generally treated as phase transitions from O3-O2 (hexagonal-monoclinic) and O2-O1 (monoclinic-hexagonal) [25–28]. In the 2nd cycle, a redox appears at 3.94/3.86 V with degradation compared with the 1st cycle. For 1 wt.% MgF_2-coated $LiCoO_2$, all redox couples at 3.93/3.89 V, 4.07/4.05 V and 4.17/4.15 V can be clearly distinguished, with narrow and sharp peaks, indicating fast lithium diffusion and better structural reversibility. The improved structural stability of cathode material can be ascribed to the physical separation by MgF_2 layer between electrolyte and electrode material, plausibly preventing the dissolution of Co^{4+} ions and further enhancing the structural stability.

It is widely accepted that the difference between redox pairs (D-value) relates to the degree of polarization [29]. Table 2 compares the D-values of pristine and 1 wt.% MgF_2-coated $LiCoO_2$ electrodes for each redox in the first two cycles. Unexceptionally, the D-values of 1 wt.% MgF_2-coated $LiCoO_2$ are smaller than those of pristine electrode, implying that MgF_2 surface modification effectively decreases the electrode polarization. Surprisingly, as a chemical and electrochemical inactive material, the MgF_2 coating layer outside bulk $LiCoO_2$ plays a positive role in surface ion transportation, which will be further explored and explained in the following EIS and FTIR analysis.

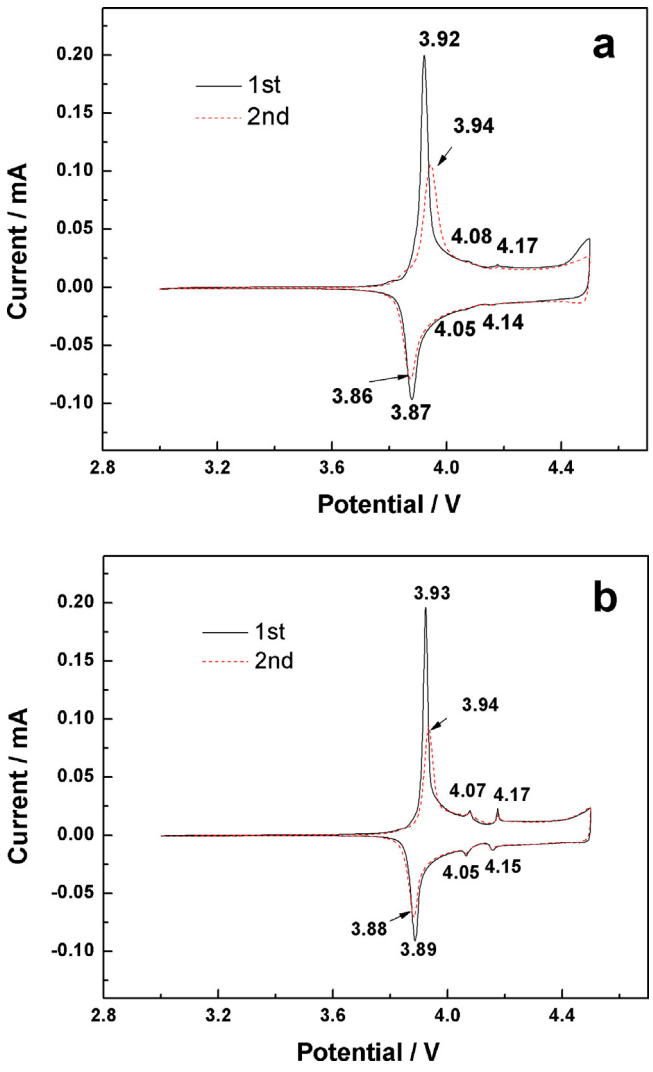

Fig. 6. Cyclic voltammograms of pristine (a) and 1 wt.% MgF_2-coated $LiCoO_2$ (b).

Table 3
R_{sf} data of the pristine and 1 wt.% MgF_2-coated $LiCoO_2$ electrodes.

Cycle number		1st	5th	10th	20th
R_{sf} (Ω)	pristine	80.5	280.4	306.8	372.4
	1 wt.% MgF_2	81.4	134.2	150.1	235.3

AC impedance curves of the pristine and 1 wt.% MgF_2-coated $LiCoO_2$ electrodes were measured after the cells at fully charged state (4.5 V) were aged for two days to reach equilibrium. The impedance behaviors of the pristine and 1 wt.% MgF_2-coated $LiCoO_2$ electrodes at different cycles are presented in Fig. 7. As widely accepted, the semicircle in high frequency region of Nyquist plot is attributed to the resistance of solid electrolyte interface (SEI) film (R_{sf}) that covers cathode particles [30], which is fitted and compared in Table 3. The R_{sf} for the 1 wt.% MgF_2-coated $LiCoO_2$ in the first cycle is a little higher than that for pristine $LiCoO_2$,

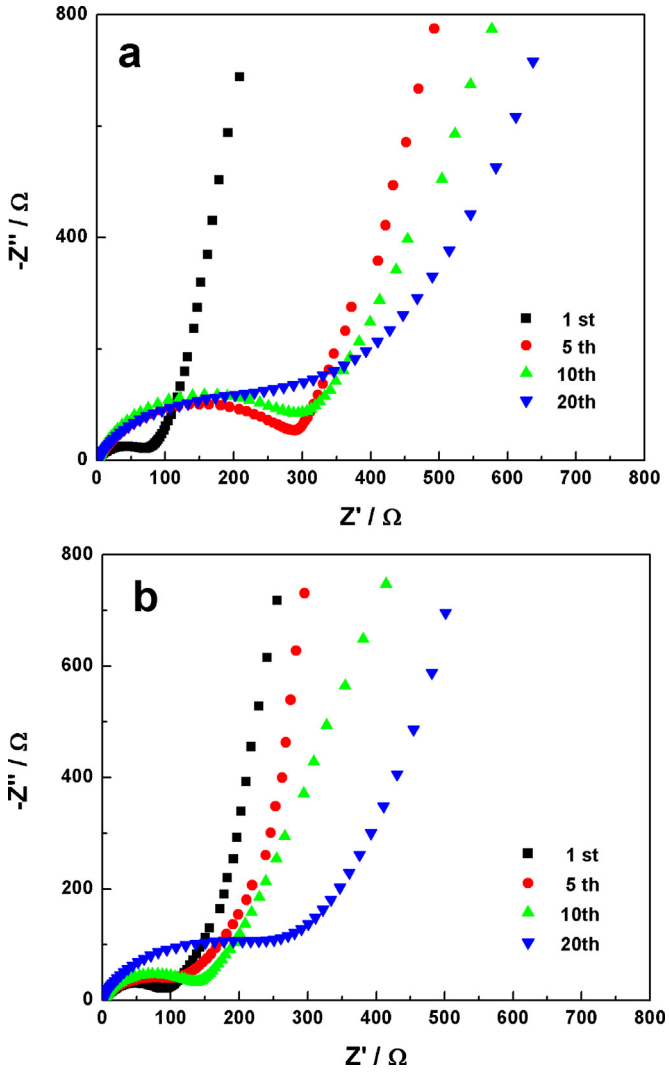

Fig. 7. Families of Nyquist plots for pristine (a) and 1 wt.% MgF_2-coated $LiCoO_2$ (b).

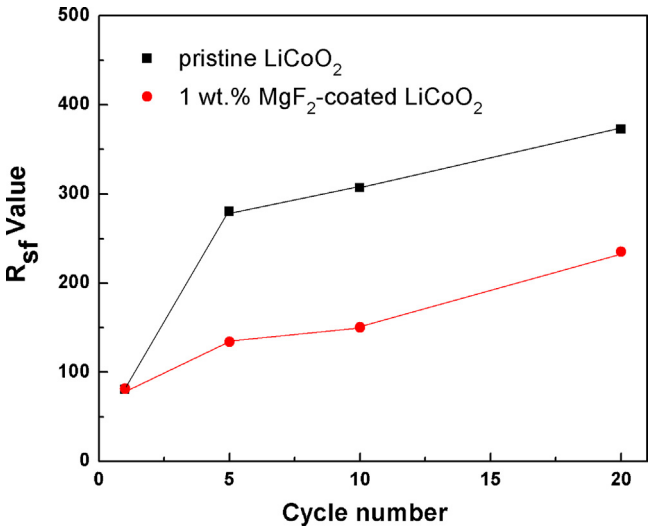

Fig. 8. Comparison of surface film resistance for the cells after different cycles.

which may be resulted from the insulating nature of MgF_2 coating layer on $LiCoO_2$. For both electrodes in Fig. 7 (a) and (b), the R_{sf} increase distinctly with cycling, which could be attributed to the increasingly precipitation of surface film. For the electrode of pristine $LiCoO_2$, the R_{sf} values in cycling increase more faster than those of 1 wt.% MgF_2-coated $LiCoO_2$, indicating less resistive component is deposited on the surface of coated $LiCoO_2$ in electrochemical cycling.

To further compare the growth of SEI film for the two electrodes, the evolutions of the impedances with cycling are demonstrated in Fig. 8. For the pristine $LiCoO_2$, the R_{sf} of the 20th cycle is about 5 times than that of the first cycle, while the R_{sf} of 1 wt.% MgF_2-coated $LiCoO_2$ increase very little. Aurbach et al. reported that the precipitation of surface film on $LiCoO_2$ positive electrode increases the electrode impedance and thereby deteriorates the capacity [31]. The pristine $LiCoO_2$ particles are covered with surface film, which is mainly composed of decomposition of electrolyte [32,33]. However, the MgF_2 layer protects the electrode surface against HF attack. The smaller R_{sf} is in favor of rapid electrochemical reactions and may result in better electrochemical performance of the active materials [34]. In this work, MgF_2 coating layer helps to alleviate the dissolution of Co^{4+} and diminish the precipitation of resistive components. Compared with the pristine $LiCoO_2$, the 1 wt.% MgF_2-coated $LiCoO_2$ exhibits smaller R_{sf}, which partly explains the improved electrochemical performances after MgF_2 coating in Figs. 4 and 5.

Fig. 9 presents the FTIR spectra of pristine and 1 wt.% MgF_2-coated $LiCoO_2$ before and after cycling. Two vibrations at 615 and 525 cm^{-1} are apparent in all the four profiles, which could be ascribed to the asymmetric stretching of Co-O bonds in CoO_6 octahedrons and the bending modes of O-Co-O bonds [35], respectively. A weak band at 1634 cm^{-1} is attributed to the ambient O-H vibration. Compared Fig. 9(a) and (c), no characteristic vibration corresponding to Mg-F appears after MgF_2 surface modification, which possibly derives from its low content. As can be observed in Fig. 9(b) and (d), new absorption peaks appear after 10 cycles. Based on the previous literatures [36–42], detailed assignments of all the new absorption peaks are listed in Table 4, wherein all the seven absorption peaks can be assigned to certain components of SEI. Strictly, the absorption peaks at 615 cm^{-1} for pristine and 1 wt.% MgF_2-coated $LiCoO_2$ after 10 cycles have been normalized in Fig. 9(b) and (d) to compare the intensities of new absorption peaks. Obviously, it is clear that 1 wt.% MgF_2 coating layer effectively suppresses the growth of the SEI film, which is consistent with the EIS results in Figs. 7 and 8. The MgF_2 hinders the

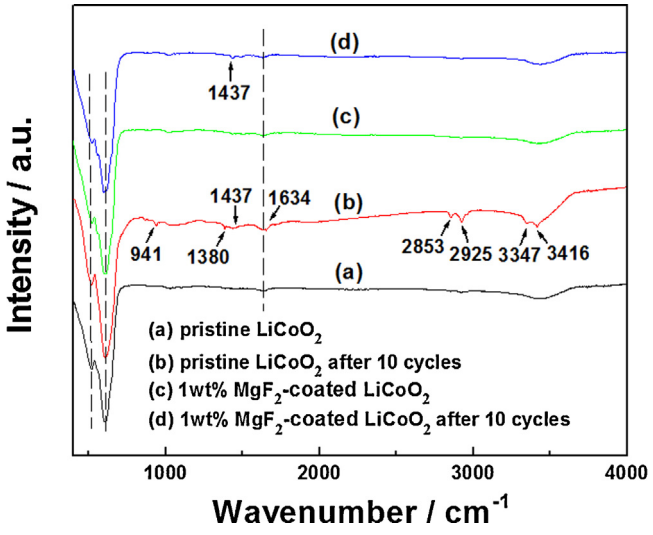

Fig. 9. FTIR spectra of the bare and 1 wt.% MgF_2-coated $LiCoO_2$.

Table 4
New infrared peaks and the corresponding identifications.

Peak position	Assignment
941	=C-H, characteristic of PEO [36] 1380 COO^- bending [37–39]
1437	Li_2CO_3, CH, CH_3 asym. bend of SEI [36,40]
2853	C-H stretching [41]
2925	C-H stretching [41]
3347	Structural OH groups [42]
3416	Structural OH groups [42]

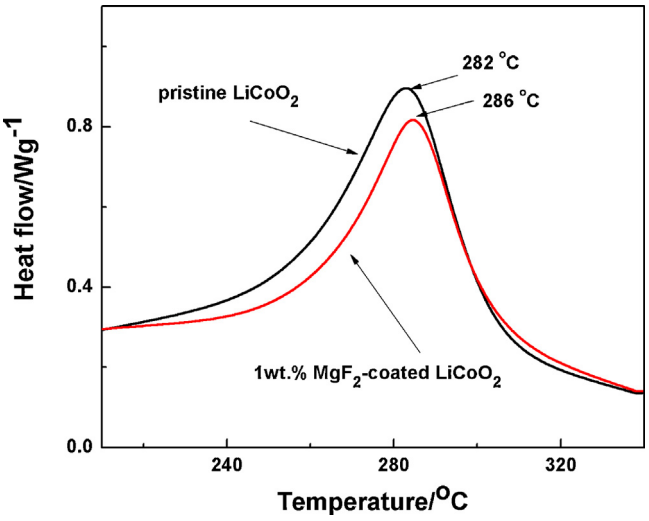

Fig. 10. DSC traces of pristine and 1 wt.% MgF_2-coated $LiCoO_2$ electrodes at charged state of 4.5 V at a heating rate of 5 °C min^{-1}.

decomposition of the electrolyte at the particle surface in repeated cycling, thus inhibits the growth of SEI film.

Thermal stability of electrodes materials is important to large-scale commercial applications of LIBs and the superior thermal stability of electrode will greatly contribute to desirable thermal stability of a cell. DSC measurement was performed to compare the thermal stabilities of delithiated pristine and 1 wt.% MgF_2-coated $LiCoO_2$ materials (Fig. 10). For 1 wt.% MgF_2-coated $LiCoO_2$, the exothermic peak shifts to a higher temperature of 286 °C compared with 282 °C for the pristine material. On the other hand, the amount of exothermic heat released is smaller in comparison with that of pristine electrode. Peak fitting to the DSC traces demonstrates that the integrated area of the exothermic peak is 85% that of pristine $LiCoO_2$ for the 1 wt.% MgF_2-coated material.

The DSC results showed significant exothermic reaction delay and heat reduction after MgF_2 surface coating, indicating the lowered reactivity with the electrolyte. This implies that the crucial factor governing the exothermic reaction is the interfacial reaction with the electrolyte and cathode. It is also believed that the strong-bonded nature of Mg-F contributes to a strong resistance to the reaction with the electrolyte, and MgF_2 has been reported to be thermally stable [43].

4. Conclusions

Different contents of MgF_2 were coated on as-prepared $LiCoO_2$ via simple chemical deposition method. Experimental results show that 1 wt.% MgF_2-coated $LiCoO_2$ cathode exhibits the optimal electrochemical performances. The homogeneous MgF_2 surface coating layer on $LiCoO_2$ separates the direct contact between electrolyte and high active electrode in deep charged state, thus alleviates the invasion of high oxidation Co^{4+} and inhibits the fast growth of SEI layer in cycling. As a result, the structural stability, cycling capability and thermal stability of $LiCoO_2$ are greatly enhanced, even at high cutoff voltage of 4.5 V. Surface modification by MgF_2 is an effective way to improve the electrochemical performances and thermal stability of $LiCoO_2$ at high cutoff voltage.

Acknowledgements

This work was supported by the National Natural Science Foundation of China (50902044), the China Postdoctoral Foundation (2013M530334), the Henan Postdoctoral Foundation (2011014), the Program for Innovative Research Team in Science and Technology in University of Henan Province (IRTSTHN) (2012IRTSTHN004) and the Innovation Scientists and Technicians Troop Construction Projects of Henan Province (124200510004).

Appendix A. Supplementary data

Supplementary material related to this article can be found, in the online version, at http://dx.doi.org/10.1016/j.electacta.2014.04.155.

References

[1] Y. Ou, J.J. Wen, H.P. Xua, S.H. Xie, J.Y. Li, J. Phys. Chem. Solids 74 (2013) 322–327.
[2] X.X. Zuo, C.J. Fan, X. Xiao, J.S. Liu, J.M. Nan, J. Power Sources 219 (2012) 94–99.
[3] Y.K. Sun, S.W. Cho, S.T. Myung, K. Amine, J. Prakash, Electrochim. Acta 53 (2007) 1013–1019.
[4] J.M. Tarason, M. Armand, Nature 414 (2001) 35–39.
[5] K. Xu, Chem. Rev. 104 (2004) 43–48.
[6] F. Zhou, X.M. Zhao, A.V. Bommel, X. Xia, J.R. Dahn, J. Electrochem. Soc. 158 (2011) 81–87.
[7] Y. Kim, G.M. Veith, J. Nanda, R.R. Unocic, M. Chi, N.J. Dudney, Electrochim. Acta 56 (2011) 65–73.
[8] T. Yang, N. Zhang, Y. Lang, K. Sun, Electrochim. Acta 56 (2011) 4058–4064.
[9] L. Yang, T. Markmaitree, B.L. Lucht, J. Power Sources 196 (2011) 22–26.
[10] Y.N. Xu, D.W. Song, J. Li, L. Li, Electrochim. Acta 85 (2012) 352–357.
[11] L.A. Riley, S.V. Atta, A.C. Dillon, S.H. Lee, J. Power Sources 196 (2011) 13–17.
[12] Y. Bai, Q.J. Chang, P. Yu, Q. Yu, S. Zhao, Y.Q. Yang, K. Jiang, Electrochim. Acta 112 (2013) 414–421.
[13] Y.K. Sun, J.M. Han, S.T. Myung, S.W. Lee, K. Amine, Electrochem. Commun. 8 (2006) 8–11.
[14] Y. Bai, Y.F. Yin, N. Liu, B.K. Guo, H.J. Shi, J.Y. Liu, J. Power Sources 174 (2007) 328–334.
[15] H.J. Lee, S.B. Kim, Y.J. Park, Nanoscale Res. Lett. 4 (2012) 7–16.
[16] Y. Cho, J. Eom, J. Cho, J. Electrochem. Soc. 157 (2010) A617–A624.
[17] H.J. Lee, Y.J. Park, Solid State Ionics 230 (2013) 86–91.
[18] Z. Quan, T.K. Osokoshi, N.K. Sonoyama, J. Alloy. Compd. 541 (2012) 137–143.
[19] M. Mladenov, R. Stoyanova, E. Zhecheva, S. Vassilev, Electrochem. Commnu. 3 (2001) 410–416.
[20] F.M. Courtel, S. Niketic, D. Duguay, Y. Abu-Lebdeh, I.J. Davidson, J. Power Sources 196 (2011) 21–28.
[21] K.S. Tan, M.V. Reddy, G.V.S. Rao, B.V.R. Chowdari, J. Power Sources 147 (2005) 241–248.
[22] Z.X. Wang, Z. Haung, L.Q. Chen, J. Electrochem. Soc. 151 (2004) A1641–A1652.
[23] N. Liu, H. Li, Z.X. Wang, X.J. Huang, L.Q. Chen, Electrochem. Solid-State Lett. 9 (2006) A328–A331.
[24] C.C. Li, Y.W. Wang, J. Power Sources 227 (2013) 204–210.
[25] T. Fang, J.G. Duh, Surf. Coat. Tech. 201 (2006) 1886–1893.
[26] H. Yamada, T.S. Suzuki, T. Uchikoshi, M. Hozumi, T. Saito, Y. Sakka, J. Eur. Ceram. Soc. 33 (2013) 1037–1044.
[27] X. Lu, Y. Sun, Z.L. Jian, X.Q. He, L. Gu, Y.S. Hu, H. Li, Z.X. Wang, W. Chen, X.F. Duan, L.Q. Chen, J. Maier, S. Tsukimoto, Y. Ikuhara, Nano Lett. 12 (2012) 6192–6197.
[28] G.T.K. Fey, C.Z. Lu, T.P. Kumar, P. Muralidharan, A.S.T. Chiang, J. Phys. Chem. Solids 67 (2006) 2337–2344.
[29] L. Maugeri, L. Simonelli, A. Iadecola, B. Joseph, M. Okubo, I. Honma, H. Wadati, T. Mizokawa, N.L. Saini, J. Power Sources 229 (2013) 272–276.
[30] T. Hutzenlaub, S. Thiele, R. Zengerle, C. Ziegler, Electrochem. Solid-State Lett. 15 (2012) 30–33.
[31] T. Hutzenlaub, A. Asthana, J. Becker, D.R. Wheeler, R. Zengerle, S. Thiele, Electrochem. Commun. 27 (2013) 77–80.
[32] L.C. Zeng, C.L. Fan, Y. Asian, New. J. Chem. 25 (2013) 3553–3556.
[33] H. Koga, L. Croguennec, P. Mannessiez, F. Weill, L. Bourgeois, M. Duttine, J. Phys. Chem. 116 (2012) 34–41.
[34] C.H. Huang, S.X. Zhuang, F.Y. Tu, J. Electrochem. Soc. 160 (2013) A376–A382.
[35] N.K. Yabuuchi, K.Y. Yamamoto, K.H. Yoshii, I. Nakai, T.S. Nishizawa, A. Omaru, T.H. Toyooka, S.C. Komaba, J. Electrochem. Soc. 160 (2013) A39–A45.
[36] Z.X. Wang, X.J. Huang, L.Q. Chen, J. Electrochem. Soc. 151 (2004) A1641–A1652.

[37] Y. Ein-Eli, B. Markovsky, D. Aurbach, Y. Carmeli, H. Yamin, S. Luski, Electrochim. Acta 39 (1994) 2559–2569.
[38] Y. Ein-Eli, D. Aurbach, Langmuir 8 (1992) 1845–1850.
[39] P. Verma, P. Maire, P. Novák, Electrochim. Acta 55 (2010) 6332–6341.
[40] X.R. Zhang, R. Kostecki, T.J. Richardson, J.K. Pugh, P.N. Ross Jr., J. Electrochem. Soc. 148 (2001) A1341–A1345.
[41] V.W. Behrendt, G. Gattow, M. Drager, Z. Anorg. Allg. Chem. 397 (1973) 237.
[42] L. Predoanâ, A. Barâu, M. Zaharescu, H. Vassilchina, N. Velinova, B. Banov, A. Momchilov, J. Eur. Ceram. Soc. 27 (2007) 1137–1142.
[43] X.W. Sun, T. Song, X.P. Wei, W.L. Quan, X.B. Liu, W.F. Su, Mater. Res. Bull. 52 (2014) 151–157.